Green synthesised-gold nanoparticles in photothermal therapy of breast cancer

Yiing Yee Foo[1], Wen Shang Saw[2], Vengadesh Periasamy[3], Wu Yi Chong[4], Sri Nurestri Abd Malek[1], Saad Tayyab[1,5] ✉

[1]Institute of Biological Sciences, Faculty of Science, University of Malaya, Kuala Lumpur, 50603, Malaysia
[2]Department of Pharmacy, Faculty of Medicine, University of Malaya, Kuala Lumpur, 50603, Malaysia
[3]Low Dimensional Materials Research Centre (LDMRC), Department of Physics, Faculty of Science, University of Malaya, Kuala Lumpur, 50603, Malaysia
[4]Photonics Research Centre, Faculty of Science, University of Malaya, Kuala Lumpur, 50603, Malaysia
[5]Centre of Research for Computational Sciences and Informatics for Biology, Bioindustry, Environment, Agriculture and Healthcare (CRYSTAL), University of Malaya, Kuala Lumpur, 50603, Malaysia
✉ *E-mail: saadtayyab2004@um.edu.my*

Published in Micro & Nano Letters; Received on 12th September 2018; Revised on 22nd October 2018; Accepted on 3rd January 2019

In this work, the use of gold nanoparticles (AuNPs), synthesised using *Curcuma mangga* (CM) extract in photothermal killing of breast cancer (MCF-7) cells is demonstrated. CM-AuNPs showed higher photothermal heating efficiency compared to citrate-AuNPs upon irradiation with a 532 nm laser. In addition, treatment of MCF-7 cells with CM-AuNPs coupled with laser irradiation for 120 s was found to significantly reduce (72%) the cell viability compared to about 13%, obtained with citrate-AuNPs. Results from flow cytometry showed that the CM-AuNP-dependent photothermal-induced MCF-7 cells death was triggered mainly by apoptosis mechanism. All these results suggested the potential use of CM-AuNPs as therapeutic agents in cancer therapy.

1. Introduction: Cancer remains as one of the major causes of death despite recent advancement in cancer treatment [1]. Photothermal therapy has emerged as an alternative approach for non-invasive cancer therapy, which employs heat generated from the conversion of photon energy, for localised destruction of cancer cells. Heating sources such as near-infrared (NIR) or visible lights are commonly used in conjunction with a photothermal agent to increase the temperature at the targeted site for the killing of cancer cells [2]. Cancer cells are usually found to be more sensitive to heat than normal cells due to the more hypoxic, acidic and nutrient-deficient microenvironment of the tumour [3, 4]. Photothermal therapy allows selective thermal ablation of cancer cells while producing a minimal effect on the normal cells in the vicinity of the tumour.

Among the various photothermal agents, gold nanoparticles (AuNPs) have been extensively employed in photothermal therapy due to their unique physicochemical properties including surface plasmon resonance (SPR). SPR of AuNPs is responsible for the strong light absorption in the visible wavelengths, which is four to five times greater than the conventional photoabsorbing dyes [5]. Therefore, effective photothermal therapy can be performed with relatively lower laser energies [6], thus minimising damage to the normal tissues in the vicinity. In addition, AuNPs are photostable and therefore, alleviate the problems encountered when using conventional photoabsorbing dyes, which are susceptible to photobleaching [7].

Although NIR laser of wavelength 808 nm has also been employed for photothermal therapy, this treatment always involves the use of gold nanorods [8, 9], which have been found more toxic to cells compared to spherical AuNPs [10, 11]. Despite much progress over the years in this field, development of stable and biocompatible AuNPs for clinical applications has remained a challenge. Aggregation of chemically synthesised AuNPs, including citrate-AuNPs in the buffer has been reported in an earlier study [12], which can limit their use for *in vivo* human applications. In addition, a commonly used stabilising agent for gold nanorods, cetyltrimethylammonium bromide has been found to be highly toxic to cells. As such, it becomes a pre-requisite to overcoat these AuNPs with selected polymers to reduce their toxicity [13]. On the other hand, smaller spherical AuNPs are found to be easier to synthesise, less toxic and possess high photoconversion capability, which enables them to be heated using standard surgical green lasers. In our previous report, we have successfully synthesised highly stable and biocompatible *Curcuma mangga* (CM)-AuNPs using CM extract [14]. The interaction of CM-AuNPs with human serum albumin has also been characterised [15]. This Letter employed these CM-AuNPs as photothermal agent and interrogated their photothermal heating efficiency as well as photothermal effects on breast cancer (MCF-7) cells. Furthermore, the mechanism of photothermal induced-cell death of MCF-7 cells treated with CM-AuNPs was also investigated.

2. Materials and methods

2.1. Materials: Gold (III) chloride trihydrate ($HAuCl_4{\cdot}3H_2O$), AuNPs (20 nm, stabilised in citrate buffer) and 3-(4,5-dimethyl-2-thiazolyl)-2,5-diphenyltetrazolium bromide (MTT) were purchased from Sigma-Aldrich Co., USA. Human breast cancer cell line (MCF-7) was obtained from American Type Culture Collection, USA. Fetal bovine serum (FBS) and Dulbecco's modified Eagle's medium (DMEM) with and without phenol red were procured from Nacalai, Japan. Fluorescein isothiocyanate-Annexin V (FITC-AV) apoptosis detection kit was supplied by BD Biosciences, USA. CM rhizome powder was obtained from Yogjakarta, Indonesia.

2.2. Preparation of AuNPs: CM-AuNPs were synthesised using CM extract according to the previously published protocol, utilising $HAuCl_4$ as the precursor and CM extract as a reducing agent [14]. These CM-AuNPs were suspended in FBS-supplemented DMEM medium (without phenol red) for photothermal studies to avoid optical interference from phenol red due to the overlap of their absorption bands. Citrate-AuNPs were also suspended in the same way.

2.3. Photothermal heating curves: Photothermal heat generation with CM-AuNPs was studied using a Spectra-Physics Millennia

doi: 10.1049/mnl.2018.5557

Prime continuous wave diode-pumped solid-state laser with a laser wavelength of 532 nm. The temperature change of the samples during laser irradiation was monitored using an Omega type T thermocouple. The thermocouple microprobe was submerged in 100 µl of the sample, placed in a 96-well plate, followed by irradiation with a laser intensity of 3 W/cm^2. Each well in the 96-well plate contained either CM-AuNPs at different concentrations (5, 10 and 20 µg/ml) or 20 µg/ml of citrate-AuNPs or DMEM medium without AuNPs as a negative control. The temperature increase in the medium was recorded for 300 s with 30 s intervals. In a separate experiment, the temperature increase of the medium with 100 µl of the sample (20 µg/ml CM-AuNPs) upon laser irradiation with different intensities (1, 2 and 3 W/cm^2) was also recorded.

2.4. Cell culture and photothermal treatment: MCF-7 cells were maintained in an FBS-supplemented DMEM medium at 37°C in a CO_2 incubator. To find a suitable irradiation time for photothermal treatment, MCF-7 cells were seeded into 96-well plate at 8000 cells/well and incubated overnight for cell adherence. The medium in each well was then removed and replaced with DMEM medium (without phenol red) and irradiated with a laser intensity of 3 W/cm^2 for different time periods (60, 120, 180, 240 and 300 s). The cell viability was determined by MTT assay [16] after incubating the treated cells at 37°C for 24 h.

Cytotoxicity of CM-AuNPs to MCF-7 cells without laser irradiation was examined using the MTT assay. MCF-7 cells were seeded under similar conditions as described above and treated with CM-AuNPs of different concentrations (5, 10, 15, 20 and 25 µg/ml), followed by incubation at 37°C for 24 h before being assessed by MTT assay.

For photothermal treatment, MCF-7 cells were seeded and treated with CM-AuNPs or citrate-AuNPs in the same way as described above. The treated cells were incubated at 37°C for 3 h, followed by irradiation with a laser intensity of 3 W/cm^2 for 120 s. Finally, the cells were incubated at 37°C for another 24 h prior to MTT assay.

For AV/propidium iodide (PI) apoptosis assay, MCF-7 cells in FBS-supplemented DMEM medium were seeded into a 24-well plate at 50,000 cells/well and incubated overnight for cell adherence. The medium in each well was then replaced with DMEM medium (without phenol red) containing CM-AuNPs (20 µg/ml) or citrate-AuNPs (20 µg/ml). The treated cells were incubated and irradiated in the same way as described above before assessed by AV/PI apoptosis assay. Untreated cells and cells treated with doxorubicin (1.5 µg/ml) were also included as negative and positive controls, respectively.

2.5. AV/PI apoptosis assay: AV/ PI staining of MCF-7 cells was performed following the protocol provided by the manufacturer (BD Biosciences). Briefly, the cells were harvested, washed with cold phosphate-buffered saline and then resuspended in 1× binding buffer. This was followed by staining with AV and PI for 15 min at room temperature in the dark. The samples were analysed by flow cytometry (BD FACS Canto II cytometer) within 1 h. Quadrant statistical analysis was employed to determine the percentage of the cell population in each quadrant.

3. Results and discussion

3.1. Photothermal properties of CM-AuNPs: The effect of CM-AuNP concentrations on their photothermal heating curves upon laser irradiation ($\lambda = 532$ nm, $I = 3$ W/cm^2) for 300 s is shown in Fig. 1*a*. As can be seen from the figure, increasing the irradiation time led to a progressive increase in the temperature of the medium, which sloped off at a longer irradiation time. The temperature increase was large during the first 120 s of irradiation but progressively became smaller beyond this time. Furthermore, the temperature increase was found directly correlated with the CM-AuNPs concentrations, being higher with higher CM-AuNP concentrations. Time course of the temperature increase followed the first order kinetics as depicted in the inset of Fig. 1*a*, where the rate of the temperature increase showed a linear correlation with CM-AuNP concentration. At a fixed laser irradiation duration of 300 s, the temperature of the medium increased from the initial temperature of ∼28°C to ∼42, ∼47 and ∼54°C for samples with 5, 10 and 20 µg/ml of CM-AuNP concentrations, respectively. This concentration-dependent temperature increase was in accordance with a previous report, where the gold nanoflower structures were used as photothermal agents [17]. However, the reported value of the temperature increase was lower (∼3°C) even with a two-fold concentration of gold nanoflowers, irradiated with higher laser intensity (5 W/cm^2) [17]. On the other hand, irradiation of the medium alone (without AuNPs) under similar conditions only increased the temperature up to 38°C. Thus, the presence of CM-AuNPs in the medium resulted in the generation of more heat upon laser irradiation. On a comparative note, citrate-AuNPs (20 µg/ml) were found to increase the temperature of the medium up to 48°C compared to ∼54°C, achieved with CM-AuNPs under similar conditions. These results clearly showed that CM-AuNPs were more efficient in converting photon energy to localised heat compared to citrate-AuNPs. Therefore, CM-AuNPs possessed a better photothermal property compared to citrate-AuNPs. Lower photothermal efficiency of citrate-AuNPs can be ascribed to their lower stability in DMEM medium due to aggregation [10], which may lead to the increase in their size, thus reducing their photothermal conversion efficiency [18]. On the other hand, no such aggregation was noticed with CM-AuNPs, which explains their higher photothermal efficiency compared to citrate-AuNPs. Since the largest temperature increase was achieved with 20 µg/ml CM-AuNPs, this CM-AuNPs concentration was selected for subsequent photothermal experiments.

In order to determine the suitable laser intensity for photothermal therapy, CM-AuNPs were treated with different laser intensities for a fixed duration of 300 s. Fig. 1*b* depicts the effect of laser intensity on the heat generation characteristic of CM-AuNPs. The heating curves, obtained with CM-AuNPs (20 µg/ml) upon irradiation with different laser intensities (1, 2 and 3 W/cm^2) showed a similar trend of temperature increase with irradiation time as noted in Fig. 1*a*. Furthermore, this effect was also found to positively correlate with the laser intensity, as higher temperature increase was noticed with higher laser intensity at all times. This was in agreement with previously published reports [17, 19]. Irradiation with a laser intensity of 1 W/cm^2 increased the temperature of the medium by ∼13°C to a final value of 40°C. Increase in the medium temperature became more pronounced when the samples were irradiated with higher laser intensities (2 and 3 W/cm^2). The temperature increase was found to be 20 and 27°C when irradiated with laser intensities of 2 and 3 W/cm^2, respectively. Therefore, the laser intensity of 3 W/cm^2 was chosen for subsequent studies.

3.2. Photothermal therapy of MCF-7 cells: Before examining the photothermal killing of MCF-7 cells by CM-AuNP-coupled irradiation, laser irradiation time was optimised to ensure its safety as to produce minimal effects on the cells in the absence of CM-AuNPs. The effect of irradiation time with a laser intensity of 3 W/cm^2 on MCF-7 cell viability in the absence of CM-AuNPs can be seen from Fig. 2*a*. Since cancer cells have been shown to be more susceptible to high temperature compared to normal cells [4], it is assumed that normal cells remain unaffected by this treatment. As evident from the figure, cell viability of MCF-7 cells remained at ∼100% upon laser irradiation up to 180 s, beyond which the cell viability decreased and a ∼20% loss in cell viability was noticed upon 300 s irradiation. Therefore, irradiation time up to 180 s with 3 W/cm^2 laser intensity seems to be the 'safety threshold' for photothermal therapy. However, irradiation for 180 s led to a temperature increase up to ∼51°C (Fig. 1*b*), which is not desirable

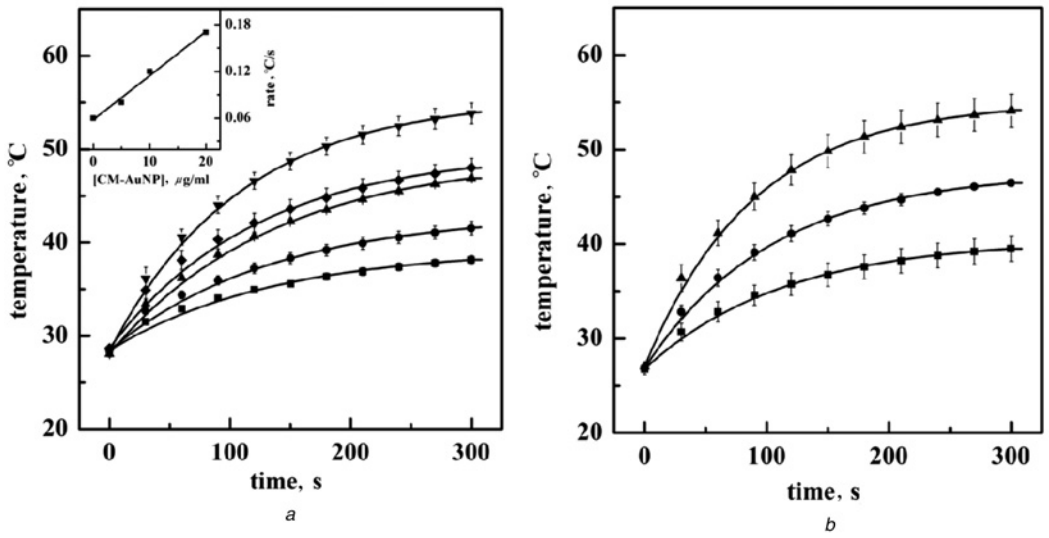

Fig. 1 *Photothermal heating curves of AuNPs upon 532 nm laser irradiation for 300 s*
a Heating curves of CM-AuNPs at different concentrations, suspended in DMEM medium, upon irradiation with laser intensity of 3 W/cm^2. Concentrations of CM-AuNPs were: 5 μg/ml (filled circle); 10 μg/ml (filled triangle) and 20 μg/ml (filled down-pointing triangle). Heating curves obtained with DMEM medium alone without CM-AuNPs (filled square) and citrate-AuNPs (black diamond suit) are also included for comparison. Inset shows the plot between rate of temperature increase and CM-AuNPs concentration
b Heating curves of CM-AuNPs (20 μg/ml), suspended in DMEM medium, upon irradiation with different laser intensities. Laser intensities used were: 1 W/cm^2 (filled square); 2 W/cm^2 (filled circle) and 3 W/cm^2 (filled triangle)

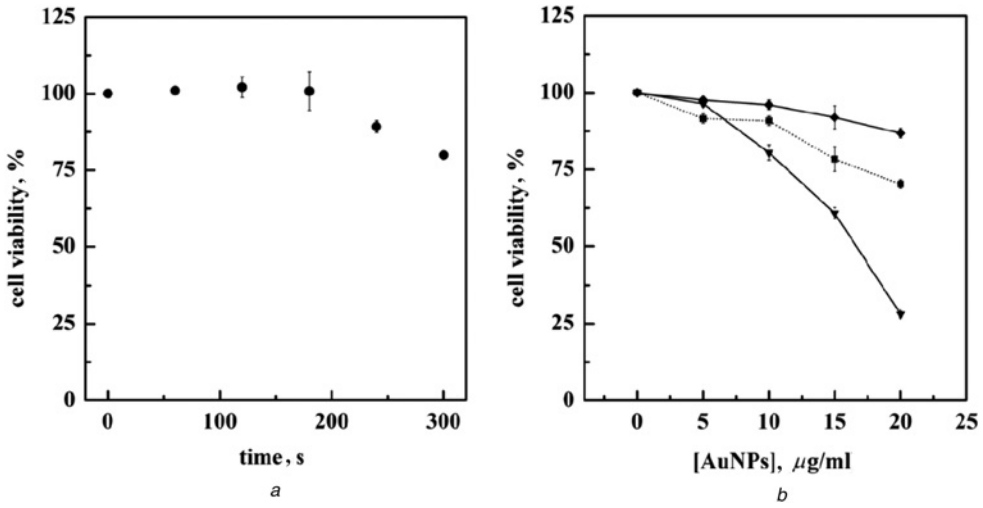

Fig. 2 *Percentage of cell viability of MCF-7 cells in DMEM medium, as analysed by MTT assay*
a Percentage of cell viability of MCF-7 cells upon irradiation with laser intensity of 3 W/cm^2 for different time periods
b Percentage of cell viability upon treatment with increasing concentrations of CM-AuNPs (▼) and citrate-AuNPs (◆), followed by irradiation with laser intensity of 3 W/cm^2 for 120 s. Percentage of cell viability after treatment with increasing concentrations of CM-AuNPs without laser irradiation (■) is also included

for photothermal treatment. It is well-known that increasing the thermal dose from 52 to 60°C can result in cell necrosis [20], which may induce inflammation [21]. To avoid this, laser irradiation duration of 120 s was selected for the photothermal treatment of MCF-7 cells in the presence of CM-AuNPs (20 μg/ml), as such treatment will increase the temperature to ~47°C (Fig. 1*b*), which is known to effectively destruct cancer cells [22].

The photothermal killing efficiency of the CM-AuNPs against MCF-7 cells was next evaluated for their potential use as a photothermal agent. Fig. 2*b* illustrates the percentage of MCF-7 cell viability after treatment with increasing concentrations of CM-AuNPs. The laser intensity and irradiation duration used were 3 W/cm^2 and 120 s, respectively. Results obtained with citrate-AuNPs under similar conditions are also included for comparison. As can be seen from Fig. 2*b*, MCF-7 cells treated with CM-AuNPs showed significantly lower cell viability under laser irradiation compared to that observed with MCF-7 cells treated with citrate-AuNPs. Treatment of MCF-7 cells with CM-AuNPs (20 μg/ml) and laser irradiation markedly reduced the cell viability to ~28%, which was significantly lower than that obtained with citrate-AuNPs treatment (~87%). In order to investigate the cytotoxicity of CM-AuNPs to MCF-7 cells without irradiation, MCF-7 cells were treated with different concentrations of CM-AuNPs but without laser irradiation and the results are included in Fig. 2*b*. About 67% cell viability was noticed upon treatment with 20 μg/ml CM-AuNPs, which was much higher than that obtained with CM-AuNP-coupled irradiation. These results suggested a greater enhancement in the cytotoxicity of

doi: 10.1049/mnl.2018.5557

CM-AuNPs upon laser irradiation, as this treatment can induce localised hyperthermia resulting in the killing of MCF-7 cells. Such an increase in the local temperature might have resulted in thermal denaturation of proteins, which may be the main factor of cell injury and cell death [23, 24]. The efficient photothermal killing of MCF-7 cells by CM-AuNPs can be attributed to their smaller size. As reported in a previous study, smaller AuNPs have been shown to be more efficient in the photothermal killing of cancer cells [25]. A comparison of the results obtained with the above treatment suggested CM-AuNPs to be a more efficient photothermal agent compared to citrate-AuNPs. Since CM-AuNPs at a concentration of 20 μg/ml were capable of reducing the viability of MCF-7 cells to ~28% and were non-toxic to normal cells [14], this concentration was chosen for apoptosis detection in the subsequent experiments.

3.3. Apoptosis detection in photothermal-induced cell death: In general, cell death mainly occurs via two mechanisms: apoptosis and necrosis [26]. Apoptosis is defined as programmed cell death, which is more advantageous compared to necrosis mainly because necrosis evokes inflammatory responses and may promote the destruction of surrounding healthy tissues [27]. Therefore, newer strategies promoting apoptosis instead of necrosis are required for cancer treatment.

In order to determine, whether CM-AuNP-coupled photothermal-induced killing of MCF-7 cells occurred mainly through apoptosis, AV/PI apoptosis assay was performed using flow cytometry. AV binds with high affinity to phosphatidylserine (PS), which is normally present in the inner leaflet of the plasma membrane. During early apoptosis, membrane asymmetry is lost, exposing PS to the outer leaflet of the plasma membrane, while retaining the membrane integrity. On the contrary, necrotic cells lose membrane integrity, thus are permeable to vital dye such as PI. Therefore, measurement of FITC-AV coupled with a dye exclusion test (PI staining) can be used to distinguish early apoptotic cells from necrotic cells, as early apoptotic cells are impermeable to PI [28].

Fig. 3*a* demonstrates dot plot of untreated MCF-7 cells (negative control), while the dot plot of MCF-7 cells taken 24 h after photothermal treatment in the presence of CM-AuNPs (20 μg/ml) is shown in Fig. 3*b*. Cell population in each quadrant represents viable cells (AV^-/PI^-), early apoptotic cells (AV^+/PI^-), late apoptotic cells (AV^+/PI^+) and dead cells (AV^-/PI^+), respectively. As evident from Fig. 3*a*, untreated cells remained viable and were populated in the lower left quadrant (AV^-/PI^-). On the contrary, the majority of the cells after photothermal treatment were

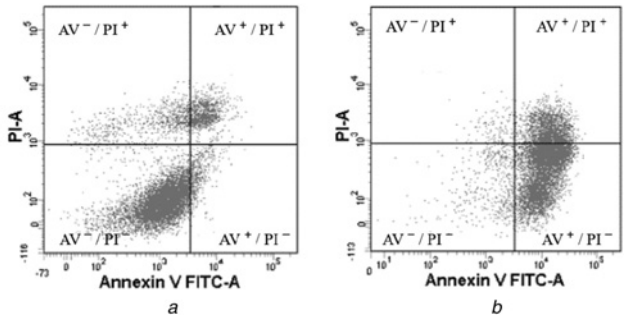

Fig. 3 *Dot plots showing flow cytometry results of AV-PI apoptosis assay for MCF-7 cells upon photothermal treatment*
Results were obtained after 24 h incubation
a Untreated MCF-7 cells (negative control)
b MCF-7 cells treated with 20 μg/ml CM-AuNPs, followed by laser irradiation (3 W/cm^2) for 120 s
The cell populations are categorised based on the four quadrants on the dot plot as viable (lower left), early apoptotic (lower right), late apoptotic (upper right) and dead cells (upper left).

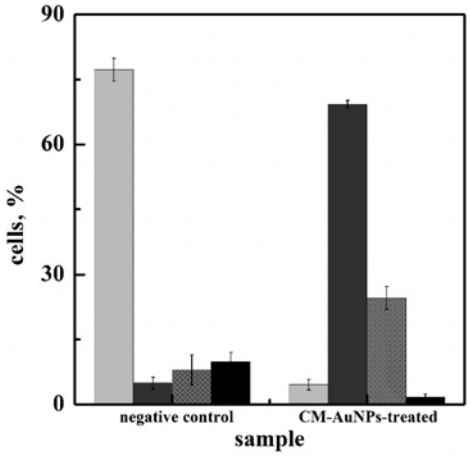

Fig. 4 *Bar diagram showing distribution of cell population in each quadrant of the dot plots, depicted in Fig. 3*
Different cell populations were: viable (▭); early apoptotic (■); late apoptotic (▨) and dead cells/debris (■)

populated in the lower right quadrant (AV^+/PI^-), characterising early apoptotic cells. In order to get a more quantitative picture, analysis of the percentage of cells in each quadrant was made and the results are shown in Fig. 4. As can be seen from the figure, the percentage of viable MCF-7 cells decreased from 77% (negative control) to 5% upon photothermal treatment with CM-AuNP. Furthermore, most of the photothermally-treated MCF-7 cells (69%) were found to be AV^+/PI^-, indicating the early phase of apoptosis, while 25% of the MCF-7 cells were noticed to be in the late apoptotic phase. The presence of late apoptotic cells in CM-AuNPs-treated MCF-7 cells can be attributed to the absence of phagocytes, which are responsible for removing the apoptotic cells [29]. In view of this, photothermal treatment with CM-AuNPs using a laser (3 W/cm^2, 120 s) triggered cell death of MCF-7 cells predominantly through apoptosis mechanism. Therefore, it could be deduced that CM-AuNPs possess great potential to be used as a photothermal agent in photothermal therapy of cancer.

4. Conclusions: This Letter has demonstrated a relatively higher photothermal heating efficiency of CM-AuNPs compared to citrate-AuNPs. Furthermore, CM-AuNPs also exhibited a remarkable photothermal therapeutic effect on MCF-7 cells upon irradiation using laser intensity of 3 W/cm^2 for 120 s. The mechanism of photothermal-induced MCF-7 cell death was found to occur mainly through apoptosis, which was preferred over necrosis cell death that commonly occurs in current photothermal treatments. Thus, the CM-AuNPs have been shown to demonstrate great potential as the photothermal agent for cancer therapy.

5. Acknowledgments: This Letter was supported by the High Impact Research (HIR) MoE grant no. UM.C/625/1/HIR/MoE/SC/02 from the Ministry of Education, Malaysia and PPP grant no. PG199-2014B from the University of Malaya. The authors also like to acknowledge the help extended by Assoc. Prof. Dr. Kiew Lik Voon in the photothermal study.

6 References

[1] Forman D., Ferlay J.: 'The global and regional burden of cancer', in Stewart B.W., Wild C.P. (Eds.): 'World cancer report 2014' (International Agency for Research on Cancer, Lyon, France, 2014), pp. 16–54
[2] Huang X., El-Sayed M.A.: 'Plasmonic photo-thermal therapy (PPTT)', *Alexandria J. Med.*, 2011, **47**, (1), pp. 1–9

[3] Luk K.H., Hulse R.M., Phillips T.L.: 'Hyperthermia in cancer therapy', *West. J. Med.*, 1980, **132**, (3), pp. 179–185
[4] Abadeer N.S., Murphy C.J.: 'Recent progress in cancer thermal therapy using gold nanoparticles', *J. Phys. Chem. C*, 2016, **120**, (9), pp. 4691–4716
[5] Huang X., El-Sayed M.A.: 'Gold nanoparticles: optical properties and implementations in cancer diagnosis and photothermal therapy', *J. Adv. Res.*, 2010, **1**, (1), pp. 13–28
[6] Link S., Burda C., Mohamed M.B., *ET AL.*: 'Femtosecond transient-absorption dynamics of colloidal gold nanorods: shape independence of the electron-phonon relaxation time', *Phys. Rev. B*, 2000, **61**, (9), pp. 6086–6090
[7] El-Sayed I.H., Huang X., El-Sayed M.A.: 'Surface plasmon resonance scattering and absorption of anti-EGFR antibody conjugated gold nanoparticles in cancer diagnostics: applications in oral cancer', *Nano Lett.*, 2005, **5**, (5), pp. 829–834
[8] Wang X., Wang H., Wang Y., *ET AL.*: 'A facile strategy to prepare dendrimer-stabilized gold nanorods with sub-10-nm size for efficient photothermal cancer therapy', *Sci. Rep.*, 2016, **6**, p. 22764
[9] Chan M.H., Chen S.P., Chen C.W., *ET AL.*: 'Single 808 nm laser treatment comprising photothermal and photodynamic therapies by using gold nanorods hybrid up conversion particles', *J. Phys. Chem. C*, 2018, **122**, (4), pp. 2402–2412
[10] Wang S., Lu W., Tovmachenko O., *ET AL.*: 'Challenge in understanding size and shape dependent toxicity of gold nanomaterials in human skin keratinocytes', *Chem. Phys. Lett.*, 2008, **463**, (1–3), pp. 145–149
[11] Zhang Y., Xu D., Li W., *ET AL.*: 'Effect of size, shape, and surface modification on cytotoxicity of gold nanoparticles to human HEp-2 and canine MDCK cells', *J. Nanomater.*, 2012, **2012**, p. 375496
[12] Wang A., Ng H.P., Xu Y., *ET AL.*: 'Gold nanoparticles: synthesis, stability test, and application for the rice growth', *J. Nanomater.*, 2014, **2014**, p. 3
[13] Alkilany A.M., Nagaria P.K., Hexel C.R., *ET AL.*: 'Cellular uptake and cytotoxicity of gold nanorods: molecular origin of cytotoxicity and surface effects', *Small*, 2009, **5**, (6), pp. 701–708
[14] Foo Y.Y., Periasamy V., Kiew L.V., *ET AL.*: '*Curcuma mangga*-mediated synthesis of gold nanoparticles: characterization, stability, cytotoxicity, and blood compatibility', *Nanomaterials*, 2017, **7**, (6), pp. 123–137
[15] Foo Y.Y., Kabir M.Z., Periasamy V., *ET AL.*: 'Spectroscopic studies on the interaction of green synthesized-gold nanoparticles with human serum albumin', *J. Mol. Liq.*, 2018, **265**, pp. 105–113
[16] Mosmann T.: 'Rapid colorimetric assay for cellular growth and survival: application to proliferation and cytotoxicity assays', *J. Immunol. Methods*, 1983, **65**, (1), pp. 55–63
[17] Song W., Gong J., Wang Y., *ET AL.*: 'Gold nanoflowers with mesoporous silica as 'nanocarriers' for drug release and photothermal therapy in the treatment of oral cancer using near-infrared (NIR) laser light', *J. Nanoparticle Res.*, 2016, **18**, (4), p. 101
[18] Jiang K., Smith D.A., Pinchuk A.: 'Size-dependent photothermal conversion efficiencies of plasmonically heated gold nanoparticles', *J. Phys. Chem. C*, 2013, **117**, (51), pp. 27073–27080
[19] Hou H., Chen L., He H., *ET AL.*: 'Fine-tuning the LSPR response of gold nanorod-polyaniline core-shell nanoparticles with high photothermal efficiency for cancer cell ablation', *J. Mater. Chem. B*, 2015, **3**, (26), pp. 5189–5196
[20] Song A.S., Najjar A.M., Diller K.R.: 'Thermally induced apoptosis, necrosis, and heat shock protein expression in three-dimensional culture', *J. Biomech. Eng.*, 2014, **136**, (7), p. 071006
[21] Rock K.L., Kono H.: 'The inflammatory response to cell death', *Annu. Rev. Pathol.*, 2008, **3**, pp. 99–126
[22] Bharathiraja S., Bui N.Q., Manivasagan P., *ET AL.*: 'Multimodal tumor-homing chitosan oligosaccharide-coated biocompatible palladium nanoparticles for photo-based imaging and therapy', *Sci. Rep.*, 2018, **8**, (1), p. 500
[23] Feng W., Chen L., Qin M., *ET AL.*: 'Flower-like PEGylated MoS2 nanoflakes for near-infrared photothermal cancer therapy', *Sci. Rep.*, 2015, **5**, p. 17422
[24] He X., Wolkers W.F., Crowe J.H., *ET AL.*: '*In situ* thermal denaturation of proteins in dunning AT-1 prostate cancer cells: implication for hyperthermic cell injury', *Ann. Biomed. Eng.*, 2004, **32**, (10), pp. 1384–1398
[25] Saw W.S., Ujihara M., Chong W.Y., *ET AL.*: 'Size-dependent effect of cystine/citric acid-capped confeito-like gold nanoparticles on cellular uptake and photothermal cancer therapy', *Colloids Surf. B, Biointerfaces*, 2018, **161**, pp. 365–374
[26] Pattani V.P., Shah J., Atalis A., *ET AL.*: 'Role of apoptosis and necrosis in cell death induced by nanoparticle-mediated photothermal therapy', *J. Nanoparticle Res.*, 2015, **17**, (1), p. 20
[27] Majno G., Joris I.: 'Apoptosis, oncosis, and necrosis: an overview of cell death', *Am. J. Pathol.*, 1995, **146**, (1), pp. 3–15
[28] Vermes I., Haanen C., Steffens-Nakken H., *ET AL.*: 'A novel assay for apoptosis flow cytometric detection of phosphatidylserine expression on early apoptotic cells using fluorescein labelled annexin V', *J. Immunol. Methods*, 1995, **184**, (1), pp. 39–51
[29] Melamed J.R., Edelstein R.S., Day E.S.: 'Elucidating the fundamental mechanisms of cell death triggered by photothermal therapy', *ACS Nano*, 2015, **9**, (1), pp. 6–11

doi: 10.1049/mnl.2018.5557